Nuclear Physics **517** (1990) 639-658
North-Holland

RELATIVISTIC COULOMB EXCITATION OF GIANT RESONANCES IN THE HYDRODYNAMICAL MODEL

A.C. VASCONCELLOS GOMES and C.A. BERTULANI

Universidade Federal do Rio de Janeiro, Instituto de Física, 21945 Rio de Janeiro, RJ-Brazil

Received 29 May 1990

Abstract: We investigate the Coulomb excitation of giant dipole resonances in relativistic heavy-ion collisions using a macroscopic hydrodynamical model for the harmonic vibrations of the nuclear fluid. The motion is treated as a combination of the Goldhaber-Teller displacement mode and the Steinwedel-Jensen acoustic mode, and the restoring forces are calculated using the droplet model. This model is used as input to study the characteristics of multiple excitation of giant dipole resonances in nuclei. Possibile signatures for the existence of such states are also discussed quantitatively.

1. Introduction

Coulomb excitation and decay of relativistic heavy ions has been extensively studied in the last years [1,2]). Traditionally, experiments have been done with activation methods to determine the cross sections for removal of few nucleons from the ions [3-5]), or by using plastic foil detectors to measure charge-changing cross sections [6,7]). More recently, the Coulomb excitation and decay of relativistic heavy ions (RHI) has been studied in exclusive experiments [8]), with improved detection techniques.

The reaction mechanism proceeds mainly via the excitation of isovector giant dipole states, although at lower beam energies ($\lesssim$1 GeV/nucleon) the isoscalar giant quadrupole also contributes significantly to the excitation cross sections [9,10]). Since the main decay modes of the giant resonance states are the particle emission channels, relativistic Coulomb excitation (RCE) is an important mechanism of nuclear fragmentation in RHI collisions, with cross sections exceeding the geometrical area of the ions for sufficiently high energies. In previous works [1-7]), it has been shown that the gross features of the available experimental data can be well explained by means of the equivalent photon method, in which the electromagnetic excitation of the projectile (or target) is obtained by folding the flux of real photons [11]), equivalent to the time dependent electromagnetic field generated by the target (projectile), with the experimentally known values of the photonuclear cross section for the respective nucleus [1,12]). Semiclassical and quantum theoretical descriptions of the reaction mechanism lead to nearly the same results as the equivalent photon method [13-15]).

Nonetheless, a complete understanding of the experimental data needs knowledge about the decay channels and branching ratios for the excited nucleus, not always known from experiment. One expects that, with the advent of more detailed exclusive experiments, RCE can become a new and useful tool to investigate excitation and decay of hitherto unexplored nuclear states. The most spectacular of such are the so-called multiphonon states, obtained from multiple RCE of giant dipole states [16,17]). The excitation of multiphonon states may be viewed as the absorption by the target (projectile) of several photons from the pulse of equivalent photons generated by the relativistic projectile (target) [16]); or it can be also described as multiple excitation of a harmonic oscillator with GDR quantum energy [17]).

If the multiphonon states exist, they correspond to large-amplitude vibrations of neutrons against protons in nuclei. Although the energy deposit is small (multiples of the energy of a GDR state), such large collective motion may lead to exotic decays of the nuclei. This is a relatively cold fragmentation process, in contrast to the violent fragmentation following central collisions of RHI, in which high temperatures are achieved.

In this paper we present a study of multiphonon states by means of a hydrodynamical model for the giant resonance states. The hydrodynamical model consists in a superposition of Goldhaber-Teller and Steinwedel-Jensen vibration modes and, as shown in ref. [18]), it reproduces very well the energy of GDR states along the nuclear table, especially for heavy nuclei. Also, the widths of these states are on the average described with use of a one-body dissipation mechanism [18]). The model is purely classical, containing parameters originated from experimental information on nuclear densities and masses. Although it is questionable to use this model to describe large-amplitude vibrations as the ones we are going to discuss here, it is very useful to provide some predictions on the basic excitation and decay mechanisms of the multiphonon states.

In sect. 2 we present a calculation of the amplitudes of vibrations of GDR states in a nucleus by means of a classical description of the coupling of the electromagnetic field of a relativistic ion with the hydrodynamical fluid describing the motion of protons and neutrons in the nucleus. This permits us to obtain the respective amount of energy transferred from the electromagnetic field to the SJ and GT vibration modes, respectively. In a quantized oscillator, the excitation of multiphonon states can be deduced from the classical approach of sect. 2. The excitation probabilities of multiphonon states are obtained in sect. 3.1. An overall analysis of the decay of the multiphonon states, together with the cross sections for different decay channels, is carried out in sect. 3.2. In sect. 4 we present our summary and conclusions.

2. Coupling of the electric field with the hydrodynamical fluid

The electric field generated by a relativistic charged particle, $Z_P e$, passing by a nucleus with an impact parameter b, and velocity v, is given at the position of the

nucleus by (see fig. 1)

$$E_z = -\frac{Z_P e\gamma vt}{(b^2+\gamma^2 v^2 t^2)^{3/2}}, \qquad E_x = \frac{Z_P e\gamma b}{(b^2+\gamma^2 v^2 t^2)^{3/2}} \tag{2.1}$$

with the z-axis parallel to the particle's trajectory, and the x-axis perpendicular to it. The Lorentz factor γ is given by $\gamma = (1 - v^2/c^2)^{-1/2}$.

For $\gamma \gg 1$ these fields are of short duration and act on the protons of the target, leading to their collective motion [1]). As in ref. [18]), we assume that this motion is described in a hydrodynamical model, with an admixture of Goldhaber-Teller (GT) and Steinwedel-Jensen (SJ) modes of vibration.

In a given position $\boldsymbol{r}$ inside the nucleus, with the charge (neutron) number $Z(N)$, the velocity of the neutron fluid $\boldsymbol{v}_n$, and of the proton fluid $\boldsymbol{v}_z$, are given by

$$\boldsymbol{v}_z = \frac{N}{A}\boldsymbol{v} = \frac{N}{A}(\boldsymbol{v}_1 + \boldsymbol{v}_2), \tag{2.2a}$$

$$\boldsymbol{v}_n = -\frac{Z}{A}\boldsymbol{v} = -\frac{Z}{A}(\boldsymbol{v}_1 + \boldsymbol{v}_2), \tag{2.2b}$$

where the factors N/A and $(-Z/A)$ are used to account for the motion of the center-of-mass of the fluid, which is not of interest.

The velocity $\boldsymbol{v}_1$ of the Goldhaber-Teller fluid is, in cartesian coordinates, given by

$$\boldsymbol{v}_1 = R(\dot{\alpha}_{1x}\boldsymbol{e}_x + \dot{\alpha}_{1z}\boldsymbol{e}_z) \tag{2.3}$$

where R is the mean radius of the nucleus, $\alpha_{1x}(\alpha_{1z})$ represents the amount of the Goldhaber-Teller mode in the motion in the $x(z)$-direction, and $\boldsymbol{e}_x(\boldsymbol{e}_z)$ are the unitary vectors along those axes.

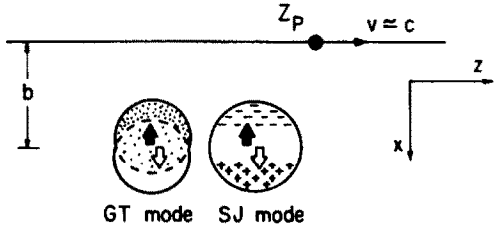

Fig. 1. A relativistic heavy ion with charge Z_P passes by a nucleus with an impact parameter b. Its electromagnetic field induces giant dipole vibrations in the nucleus, which can be described as a combination of Goldhaber-Teller and Steinwedel-Jensen vibrations. The system of axes used in the text is also shown.

The velocity v_2 of the Steinwedel-Jensen fluid at a distance r from the centre-of-mass of the fluid is, in polar coordinates, given by

$$\begin{aligned} v_2 &= \dot{\alpha}_{2x}\frac{K}{k}\left[j_1'(kr)\cos\theta e_r - \frac{1}{kr}j_1(kr)\sin\theta e_\theta\right] \\ &\quad + \dot{\alpha}_{2z}\frac{K}{k}\left[j_1'(kr)\cos\theta' e_r' - \frac{1}{kr}j_1(kr)\sin\theta' e_\theta'\right] \\ &= \frac{K}{k}\Bigg[(\dot{\alpha}_{2x}\cos\theta + \dot{\alpha}_{2z}\sin\theta\sin\phi)j_1'(kr)e_r \\ &\quad - (\dot{\alpha}_{2x}\sin\theta + \dot{\alpha}_{2z}\cos\theta\sin\phi)\frac{1}{kr}j_1(kr)e_\theta - \dot{\alpha}_{2z}\cos\phi\frac{1}{kr}j_1(kr)e_\phi\Bigg], \end{aligned} \tag{2.4}$$

where $\theta(\theta')$ is the polar angle with respect to the symmetry axis $z(x)$, $j_1(kr)$ is the spherical Bessel function of first order, $\alpha_{2x}(\alpha_{2z})$ is the amount of Steinwedel-Jensen mode of motion in the $x(z)$-direction, and

$$kR = a = 2.081\ldots, \qquad K = \frac{2a}{j_0(a)} = 9.93\,. \tag{2.5}$$

The total kinetic energy of the system is

$$T = \tfrac{1}{2}m^*\int_V (\rho_z v_z^2 + \rho_n v_n^2)\,\mathrm{d}^3 r\,, \tag{2.6}$$

where $m^* = 0.7m_N$, with m_N equal to the nucleon mass, and $\rho_z(\rho_n)$ is the proton(neutron) density.

We use m^* instead of m_N for the nucleon mass in order to account for the fact that the effective inertia of the collective motion is somewhat smaller than the simple addition of the bare masses of protons and neutrons. This arises due to the exchange character of the nucleon-nucleon force, which allows for a charge exchange between a proton and a neutron without involving an actual displacement of then in space. The rescaling of the nucleon mass is in fact needed to reproduce the correct strength and energy position of the giant resonances [18]).

The integral over the nuclear volume can be performed analytically and written in matrix form as

$$T = \tfrac{1}{2}\dot{\underline{\alpha}}^T\cdot\underline{T}\cdot\dot{\underline{\alpha}} = \tfrac{1}{2}\sum_{ik}\dot{\alpha}_i T_{ik}\dot{\alpha}_k\,, \tag{2.7a}$$

where $\underline{\alpha}$ represents a vector whose components are the amounts of GT and SJ modes in the x and z directions, and $\underline{T}$ is the kinetic energy matrix. One finds

$$\underline{\alpha} \equiv \begin{pmatrix}\alpha_1\\ \alpha_2\\ \alpha_3\\ \alpha_4\end{pmatrix} = \begin{pmatrix}\alpha_{1x}\\ \alpha_{1z}\\ \alpha_{2x}\\ \alpha_{2z}\end{pmatrix}, \tag{2.7b}$$

$$\underline{T} = \tau \begin{pmatrix} 1 & 0 & 1 & 0 \\ 0 & 1 & 0 & 1 \\ 1 & 0 & d & 0 \\ 0 & 1 & 0 & d \end{pmatrix}, \tag{2.7c}$$

$$\tau = m^* \frac{NZ}{A} R^2, \tag{2.7d}$$

with

$$d = \tfrac{1}{2}(a^2 - 2) = 1.166. \tag{2.7e}$$

The separation of the (sharp) proton and neutron distributions, as well as the neutron excess at the surface leads to a restoring force on the relative distance of the proton and of the neutron fluid. Following ref. [18]) the restoring potential energy can be calculated in the droplet model and, for the superposed GT and SJ vibrations, one obtains

$$V = \tfrac{1}{2}\underline{\alpha}^T \cdot \underline{V} \cdot \underline{\alpha} \tag{2.8a}$$

where

$$\underline{V} = \begin{pmatrix} v_1 & 0 & v_2 & 0 \\ 0 & v_1 & 0 & v_2 \\ v_2 & 0 & v_3 & 0 \\ 0 & v_2 & 0 & v_3 \end{pmatrix} \tag{2.8b}$$

with

$$v_1 = \tfrac{2}{3}HA^{4/3}, \qquad v_2 = \tfrac{2}{3}Pa^2A,$$
$$v_3 = \tfrac{1}{4}Ja^2(a^2-2)A - \tfrac{1}{6}GA^{2/3}a^4. \tag{2.8c}$$

The droplet coefficients J, H, P and G are derived from a fit to nuclear masses and the best fit [18]) corresponds to the values 36.8, 14, 9.74 and 31.63 (in MeV), respectively.

In the droplet model, the work performed by the driving fields (2.1) in displacing the proton and neutron fluids is given by $W = W_{1x} + W_{1z} + W_{2x} + W_{2z}$, which can be written in compact form as

$$\underline{W} \equiv \begin{pmatrix} W_{1x} \\ W_{1z} \\ W_{2x} \\ W_{2z} \end{pmatrix} = qR \begin{pmatrix} \alpha_{1x}E_x \\ \alpha_{1z}E_z \\ \alpha_{2x}E_x \\ \alpha_{2z}E_z \end{pmatrix}, \tag{2.9}$$

where the dipole charge $q = eNZ/A$ accounts for the elimination of the center-of-mass motion.

To complete the hydrodynamical analysis, the attenuation of the collective vibrations can be derived by using a one-body dissipation mechanism and comparing the viscosity coefficients with the decay widths of the giant resonances, as was done

in ref. [18]). From that, one can build a Rayleigh dissipation function, which can be written as

$$\mathcal{F} = \tfrac{1}{2}\dot{\underline{\alpha}} \cdot \underline{F} \cdot \dot{\underline{\alpha}}\,, \tag{2.10a}$$

where

$$\underline{F} = f\begin{pmatrix} 1 & 0 & 1 & 0 \\ 0 & 1 & 0 & 1 \\ 1 & 0 & 1 & 0 \\ 0 & 1 & 0 & 1 \end{pmatrix}, \tag{2.10b}$$

with

$$f = mR\bar{v}\frac{NZ}{A}. \tag{2.10c}$$

In this expression $\bar{v}$ is $\frac{3}{4}$ of the Fermi velocity v_F of the nucleons.

Using eqs. (2.7)-(2.10) and the Euler-Lagrange equations of motion, one gets the equation for the damped oscillator with a driving force

$$\underline{V} \cdot \underline{\alpha} + \underline{F} \cdot \dot{\underline{\alpha}} + \underline{T} \cdot \ddot{\underline{\alpha}} = \underline{Q}\,, \tag{2.11a}$$

where

$$\underline{Q} = qR\begin{pmatrix} E_x \\ E_z \\ E_x \\ E_z \end{pmatrix}. \tag{2.11b}$$

By means of use of the Fourier transform

$$\tilde{\alpha}_i(\omega) = \frac{1}{\sqrt{2\pi}}\int_{-\infty}^{\infty} \alpha_i(t)\, \mathrm{e}^{-i\omega t}\, \mathrm{d}t \tag{2.12}$$

one can readily solve eq. (2.11), resulting for the motion in the x-direction

$$\tilde{\alpha}_{1x}(\omega) = qR\tilde{E}_x(\omega)[\tau\omega^2(1-d) - (v_2 - v_3)]\frac{1}{Q(\omega)}, \tag{2.13a}$$

$$\tilde{\alpha}_{2x}(\omega) = \frac{(v_1 - v_2)}{[\tau\omega^2(1-d) - (v_2 - v_3)]}\,\tilde{\alpha}_{1x}(\omega)\,, \tag{2.13b}$$

where

$$\begin{aligned} Q(\omega) = {} & \tau\omega^2(2v_2 - v_3 - dv_1) + (v_1 v_3 - v_2^2) \\ & - \tau^2\omega^4(1-d) + if\omega[\tau\omega^2(1-d) + (v_1 - 2v_2 + v_3)]\,. \end{aligned} \tag{2.13c}$$

The equations for $\tilde{\alpha}_{1z}$ and $\tilde{\alpha}_{2z}$ are similar to (2.13a) and (2.13b), but with $\tilde{E}_x(\omega)$ replaced by $\tilde{E}_z(\omega)$.

The Fourier transforms of the fields (2.1) are given analytically by

$$\tilde{E}_x(\omega) = \frac{Z_P e}{bv}\sqrt{\frac{2}{\pi}}\left[\frac{\omega b}{\gamma v}K_1\left(\frac{\omega b}{\gamma v}\right)\right], \tag{2.14a}$$

$$\tilde{E}_z(\omega) = -i\frac{Z_P e}{\gamma\omega b}\sqrt{\frac{2}{\pi}}\left[\frac{\omega b}{\gamma v}K_0\left(\frac{\omega b}{\gamma v}\right)\right]. \tag{2.14b}$$

As a function of ω these functions are monotonous up to $\omega_{max} \sim \gamma v/b$. After this value, they begin to decrease exponentially with ω. A good approximation for $\tilde{E}_x(\omega)$ is

$$\tilde{E}_x(\omega) \cong \begin{cases} \sqrt{2/\pi}\, Z_P e/bv, & \text{for } \omega b/\gamma v < 1 \\ 0 & \text{for } \omega b/\gamma v > 1\,. \end{cases} \tag{2.15}$$

On the other hand, the function $1/Q(\omega)$ in eqs. (2.13) has a peak at the resonant values $\omega = \omega_\pm$, where (taking $f \sim 0$)

$$\omega_\pm^2 = \frac{1}{2\tau(d-1)} \{(v_1 d + v_3 - 2v_2) \pm \sqrt{(v_1 d + v_3 - 2v_2)^2 + 4(d-1)(v_2^2 - v_1 v_3)}\}\,. \tag{2.16}$$

The energy $\hbar\omega_+$ corresponds to an antidipole vibration of the SJ against the GT fluids, nearly out of phase and whose dipole moment almost vanishes. It is of little physical interest and lies very high in energy. For a nucleus with $A = 150$, one finds $\omega_+/\omega_- \simeq 6$, where $\hbar\omega_- \simeq 15$ MeV. The energy $\hbar\omega_-$ reproduces quite well the giant resonance dipole energies along the nuclear table. In fig. 2 a plot is shown of the giant resonance energy $\hbar\omega_-$ as a function of the nuclear mass A. The data are taken from refs. [19-22]). One sees that a good agreement with the experimentally determined position of the giant resonances is obtained. In fact, $\hbar\omega_-$ reproduces correctly the experimentally observed transition from a proportionality of E_{GDR} with $A^{-1/6}$ to a proportionality with $A^{-1/3}$.

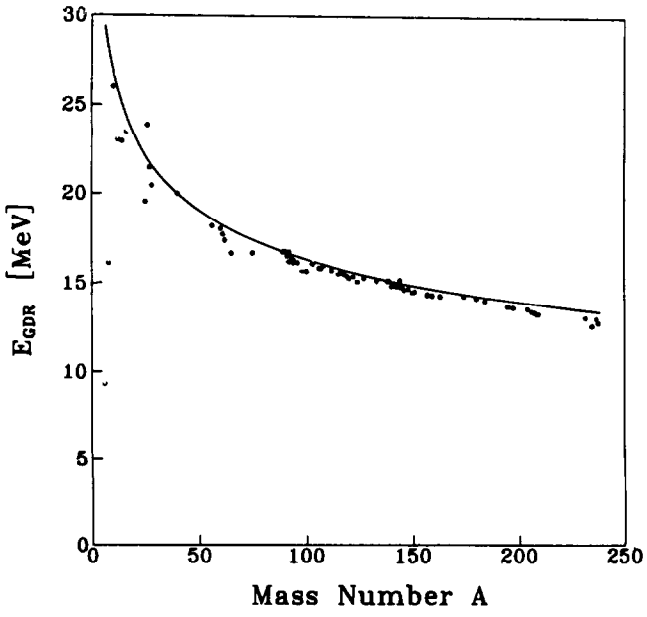

Fig. 2. Experimentally determined energy of the giant dipole resonance as a function of the nuclear mass number. The solid curve is the prediction of the droplet model represented by eq. (2.16).

From (2.13), (2.15) and (2.16) one observes that the amplitude spectra represented by $\alpha_{ix}(\omega)$ for the induced vibrations are sensitive essentially to the information if $\hbar\omega_- < \gamma\hbar c/b$, or not. For a typical relativistic Coulomb collision, with $b \simeq 15$ fm, this condition is easily fulfilled. This means that the Coulomb field of a relativistic particle is able to transfer more than sufficient energy to induce giant dipole vibrations on a target. The absorption spectra will have a form of an usual lorentzian with the strength determined by a coefficient proportional to Z_P^2.

The total energy transferred from the Coulomb field to a particular vibration mode of the hydrodynamical fluid is given by the real part of the integral over frequency, i.e.

$$\Delta E_{1x} = qR\mathcal{R}\int_{-\infty}^{\infty} i\omega\alpha_{1x}(\omega)\tilde{E}_x^*(\omega)\,\mathrm{d}\omega$$

$$= 2fq^2R^2\int_0^{\infty}\omega^2[\tau\omega^2(1-d)-(v_2-v_3)]|\tilde{E}_x(\omega)|^2$$

$$\times[\tau\omega^2(1-d)+(v_1-2v_2+v_3)]\frac{\mathrm{d}\omega}{|Q(\omega)|^2}. \qquad (2.17)$$

The corresponding expressions for ΔE_{1z}, ΔE_{2x} and ΔE_{2z} are obtained analogously.

In fig. 3 is shown a numerical calculation of (2.17) for the energy transferred to dipole vibrations in uranium in a $^{238}U+^{238}U$ collision with impact parameter $b=$ 16 fm, as a function of the laboratory energy per nucleon. For low energy collisions

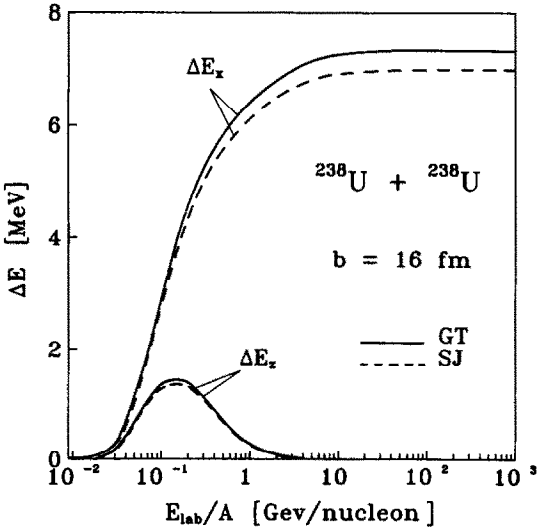

Fig. 3. Energy transferred by the electromagnetic field to giant dipole vibrations in ^{238}U as a function of the laboratory energy per nucleon for the reaction $^{238}U+^{238}U$ at $b=16$ fm. The dashed (solid) lines correspond to absorption by Steinwedel-Jensen (Goldhaber-Teller) vibration mode. The energies absorbed in the beam direction and perpendicularly to it are also displayed.

where Coulomb recoil effects are important, we used the recoil correction $b \to b + \pi Z_P Z_T e^2/2\gamma\mu v^2$, where μ is the reduced mass. This correction approximately accounts for the fact that, at the closest approach distance, the ions are somewhat more displaced from each other and the action of the electric field is somewhat weaker than it would be if the projectile would move in a straight line [13]). One observes from fig. 3 that the amount of energy transferred to the SJ and GT vibrations are approximately the same. Also, the vibration parallel to the beam axis (z-axis) only absorbs an appreciable amount of energy in intermediate energy collisions, around some hundreds of MeV per nucleon. Going higher in collision energy, the absorption goes entirely to the vibrations perpendicular to the beam axis. At very high energies, above 1 GeV/nucleon, the energy transferred to the vibration modes saturate at a constant value, and are practically independent of the damping factor f. That is when the approximation (2.15) is valid. In this case we can put $|\tilde{E}_{jx}(\omega)|^2 \simeq |E_{jx}(0)|^2$ and take it out of the integrand in (2.17). Then, the energy transferred to the vibration modes is factorized into the product of two strengths, one depending only on the projectile field, and the other one depending on the giant dipole resonance parameters.

For very high energies, the total amount of energy transferred to the SJ and GT vibrations is $\Delta E \sim \Delta E_x(\mathrm{SJ}) + \Delta E_x(\mathrm{GT})$, where ΔE_x is the energy given to vibrations perpendicular to the beam axis. This sum is about 15 MeV for $^{238}\mathrm{U} + ^{238}\mathrm{U}$ collisions at grazing impact parameter. But this is just about the energy of a giant dipole resonance state in $^{238}\mathrm{U}$. In the language of quantum mechanics, this means that the probability of exciting a giant resonance state in relativistic Coulomb collisions of heavy ions is about one. That is, if the multiphonon states exist, they are accessible by means of this excitation mechanism. An estimate of their excitation probabilities maybe obtained by extending the classical oscillator model to a quantum one, with the same underlying parameters. This naive procedure allows us to make straightforward predictions of the magnitudes of the cross sections for the excitation of these states.

3. Quantized oscillator: multiphonon states

3.1. EXCITATION PROBABILITIES

In refs. [16,17]) it has been proposed that relativistic Coulomb excitation could be a unique mechanism in order to achieve the hitherto unknown states composed by multiple excitation of giant dipole states; the so-called multiphonon states. Due to their large charges and to Lorentz contraction, relativistic heavy ions are the ideal tool to excite and investigate such states. In a simple harmonic vibrator model, the first excited state would correspond to a single giant dipole state, the second state to a double phonon state, with twice the energy of a single dipole state, and so on. In the exact theory of multiple excitation of a quantum harmonic oscillator [see,

e.g. ref. [23])] the probability to excite a $\mathcal{N}$-phonon state in a multistep process is given by a Poisson distribution

$$P_{\mathcal{N}}(b) = \frac{1}{\mathcal{N}!}\chi^{\mathcal{N}}e^{-\chi}, \tag{3.1}$$

where $\chi(b) = \langle E\rangle / E_{\mathrm{GDR}}$, with E_{GDR} equal to quantum energy and $\langle E\rangle$ the average energy transferred to the oscillator, i.e. $\langle E\rangle = \Delta E_x(\mathrm{SJ}) + \Delta E_x(\mathrm{GT}) + \cdots$. This average energy can be taken as the classical energy calculated in sect. 2 within the hydrodynamical model. In this way, we can calculate the probability to excite a multiphonon state, $P_{\mathcal{N}}(b)$, in a collision with impact parameter b.

In fig. 4, we plot the excitation probabilities of a multiphonon state in ^{238}U projectile incident on a ^{238}U target at $b = 16$ fm and as a function of the laboratory energy per nucleon. One observes that, at energies above some GeV per nucleon, the excitation probabilities become constant and that the probability to excite a two-phonon state in a grazing collision is only a factor 2–3 smaller than the probability to excite a one-phonon state. For larger impact parameters this factor increases considerably.

The saturation of ΔE_{jk} and $P_{\mathcal{N}}$ at high energies has a simple origin. The energy given to the collective vibrations of the nucleus at high energies is approximately proportional to the product of the electric field at their distance of closest approach and of the time duration of action of this field. The first quantity is proportional to γ [see. eq. (2.1)], while the second is proportional to $1/\gamma$. Therefore, the energy transferred, and consequently the excitation amplitudes, saturate at high-energy

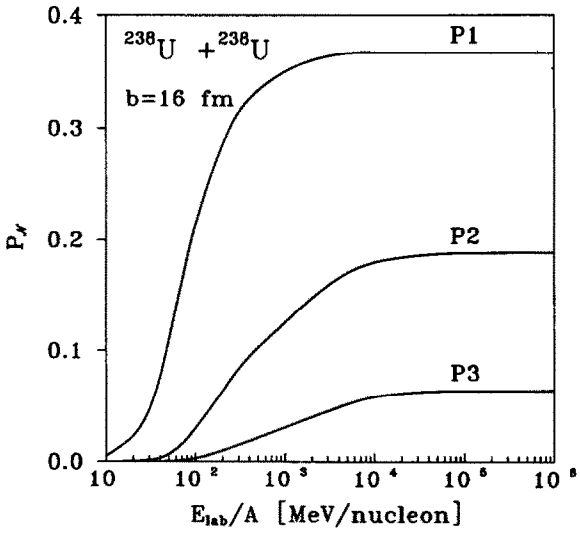

Fig. 4. Excitation probabilities of GDR multiphonon states in ^{238}U for the reaction ^{238}U+^{238}U at $b = 16$ fm and as a function of the laboratory energy per nucleon.

collisions. Due to the suddenness of the collisions, this occurs already at moderately high energies, above 1 GeV/nucleon.

If the multiphonon states exist, they correspond to large amplitude vibrations of the nuclei and would result in unusual large neutron and proton excess on the nuclear surface. Since the average separation of the center of mass of protons and neutrons grows proportionally to $\sqrt{2\mathcal{N}-1}$, in the SJ mode the local variations of the density of protons and neutrons are given by

$$\delta\rho_z = \frac{N}{A}\rho_z\delta\eta\,, \qquad \delta\rho_n = -\frac{Z}{A}\rho_n\delta\eta\,, \tag{3.2}$$

where

$$\delta\eta = \sqrt{2\mathcal{N}-1}\,\alpha_2^{(0)} K j_1(kr)\cos\theta\,, \tag{3.3}$$

with the coefficients k and K given by eq. (2.5). The quantity $\alpha_2^{(0)}$ corresponds to the amplitude of a SJ mode in an usual giant dipole resonance state. The proton and neutron densities are taken as Fermi distributions with the same radius and diffuseness parameters $R = 1.2A^{1/3}$ fm and $a = 0.65$ fm, respectively.

The GT mode corresponds to the whole displacement of the distribution of protons against that of neutrons. The distribution of protons and neutrons as a function of the distance to the center-of-mass is a combination of the SJ and GT distributions and is given approximately by

$$\rho_z = \frac{Z\rho_0[1-(N/AR)d_1^{\mathcal{N}} K j_1(kr)\cos\theta]}{A[1+\exp((|r+Nd_2^{\mathcal{N}}/A|-R)/a)]}\,, \tag{3.4a}$$

$$\rho_n = \frac{N\rho_0[1+(Z/AR)d_1^{\mathcal{N}} K j_1(kr)\cos\theta]}{A[1+\exp((|r-Zd_2^{\mathcal{N}}/A|-R)/a)]}\,, \tag{3.4b}$$

where $\rho_0 = 0.17/fm^3$, and $d_{1,2}^{\mathcal{N}} = \sqrt{2\mathcal{N}-1}\,\alpha_{1,2}^{(0)} R$. The coefficients $\alpha_{1,2}^{(0)}$ are taken from the static case, i.e., by solving (2.11a) without the driving and damping forces, as was done in ref. [18]).

We assume that we are on the high-energy regime, where only the collective vibrations perpendicular to the beam axis are important and we plot in fig. 5, for a given $\mathcal{N}$-phonon state in ^{238}U, the local neutron excess along the GDR symmetry axis, defined by

$$\delta^{(\mathcal{N})} = \frac{(\rho_n-\rho_z)}{(\rho_n+\rho_z)}\,. \tag{3.5}$$

At the nuclear surface, around $r \simeq 7$ fm, the neutron excess can be very large for high values of $\mathcal{N}$. For example, in the $\mathcal{N}=4$ state (see fig. 6) the amount of neutron excess at the surface for the uranium nucleus is about 70%, while the average value in the whole nucleus is 23%. The large separation between proton and neutron distributions in a multiphonon state suggests that the multiphonon states will have very unusual decays and that the nucleus will fragment into exotic pieces rich in

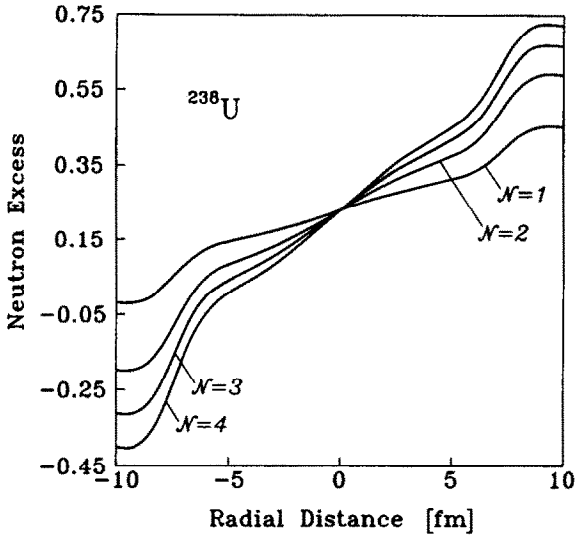

Fig. 5. Relative neutron excess along the symmetry axis of a GDR multiphonon state in ^{238}U at the moment of largest separation between protons and neutrons and as a function of the distance to the center-of-mass of the nucleus.

neutrons, like tetraneutrons, ^{8}He, ^{11}Li, etc. In contrast to the violent frontal collisions with relativistic heavy ions, such fragmentation modes would prosecute via small energy deposits of order of 30, 45, or 60 MeV (cold fragmentation). These fragments would move at the same velocity as the projectile nucleus and could be used in secondary beam experiments.

A more efficient way of inducing large collective motions in heavy ions is by means of channelling in crystals. Channelling occurs due to the coherent action (on a projectile) of the electromagnetic field of a string of nuclei in a crystal (see fig. 7). If the beam axis coincides with that of a periodic row of nuclei, there will be a resonant behavior of the energy transferred to the projectile in its own referential.

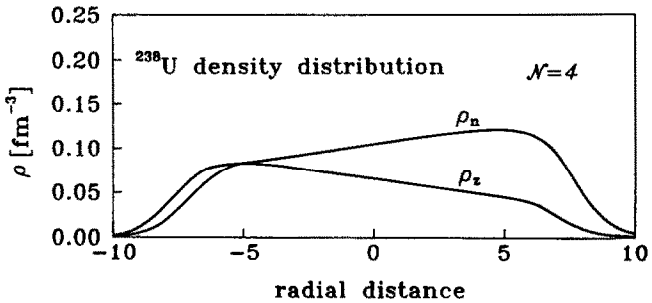

Fig. 6. Proton and neutron density distributions at the moment of largest separation between them in a $\mathcal{N}=4$ multiphonon state in ^{238}U.

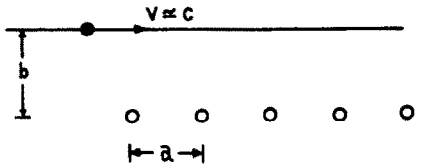

Fig. 7. Passage of a projectile nucleus with impact parameter b by a string of atomic sites in a crystal. For certain values of the periodic separation between neighboring nuclei a, and of the Lorentz factor γ, the energy transferred to giant dipole vibrations in the projectile will be resonant.

This resonant peak occurs when the transit time between neighboring nuclei, separated by a lattice spacing a, coincides with a multiple l of the period of a collective dipole motion, that is

$$\frac{\omega a}{\gamma c} = 2\pi l, \tag{3.6}$$

with $l = 0, 1, 2, 3, \ldots$ The value $l = 0$ also corresponds to a resonant behavior and means $\gamma \to \infty$, i.e., the projectile is so fast that it gets almost instantaneously the Coulomb "kicks" transferred by each of the nucleus in the lattice string.

The total energy transferred by a lattice string to a projectile passing with impact parameter b may be easily calculated in the hydrodynamical model. For a crystal axis with M nuclei the electric fields in (2.1) must be replaced by

$$E'_j(t) = \sum_{k=1}^{M} E_j(t + ka/\gamma v)\,. \tag{3.7}$$

Instead of (2.14) the Fourier transforms of the electric fields will be

$$\tilde{E}'_j(\omega) = \exp\left[i(M-1)\omega a/2\gamma v\right] \frac{\sin\left(M\omega a/2\gamma v\right)}{\sin\left(\omega a/2\gamma v\right)} \tilde{E}_j(\omega), \tag{3.8}$$

which have resonant peaks when the frequency ω matches the condition (3.6).

Inserting (3.8) into (2.17) we can calculate the total energy transferred to a projectile nucleus after passing M target nuclei in the crystal. The most interesting situation is of course when the condition (3.6) is fulfilled. For a typical crystal, $a \sim 2$ Å, and for $\gamma = 200$ (beam energy available at CERN), the resonant energy will be equal to the giant dipole energy for $l = 1$. This means that, after passing the first nucleus in the periodic string, the projectile is excited to a GDR state, then it vibrates once, is excited to a 2-phonon state after passing by the second nucleus in the string, vibrates twice, is excited to a 3-phonon state, etc. Such a picture is only valid if the width of these collective states are much smaller than their energy separation. At a certain point the energy transferred to the projectile is so large that it disintegrates before passing by other nuclei in the string.

3.2. FRAGMENTATION MODES

The GDR multiphonon states are very collective, with neutrons and protons having a net momentum along the symmetry axis. But the average momentum per proton (or neutron) along the symmetry axis is very small compared to the Fermi momentum. Even in a $\mathcal{N}=4$ state, each nucleon would have an average momentum of 20 MeV/c, assuming that the energy of the $\mathcal{N}$-phonon state is shared equally to all nucleons moving along the same axis. In such case the Goldhaber statistical model of fragmentation [24]) may give good estimates of the momentum distribution of the final fragments. This model assumes that the average momentum of a certain fragment is nearly the sum of the individual momenta of the nucleons of a piece of the nucleus with the same number of nucleons as the fragment. The momentum distribution of the fragments, in the frame of reference of the nucleus, is assumed to be a gaussian (except for protons for which an exponential distribution is assumed). Using the Thomas–Fermi model for the nucleus, the half-width of the gaussian is found to be given by [24])

$$\Delta^2=\frac{1}{5}\frac{K(A-K)}{A-1}p_{\mathrm{F}}^2, \tag{3.9}$$

where $A(K)$ is the mass number of the nucleus (fragment) and p_{F} is the Fermi momentum of the nucleus, which is about 250 MeV/c for heavy nuclei. The model has application in peripheral heavy-ion collisions and is able to fit the experimental data over a wide range. For example, for nucleon, deuteron or α-emission one obtains from (3.9) the values 114, 160 and 226 MeV/c, respectively, for the momentum width of the distribution. It has been shown that Pauli corrections [25]) and phase-space constraints [26,27]) not included in the Goldhaber model would decrease the value of Δ, but not much. Therefore, the values cited above should be essentially what one also expects for the fragmentation of multiphonon states.

In principle, one might think that the decay of the multiphonon states should have close resemblance with the decay modes of photo-induced reactions. The decay mechanism at high photon energies (~30–100 MeV) develops mostly through two distinct steps: (a) the energy is absorbed by a pair of nucleons (quasi-deuteron effect) followed by the emission of a fast nucleon in a cascade process; (b) a compound nucleus is left behind, and competition between nucleon evaporation and fission becomes the dominant mechanism [28]). But a multiphonon state represents the simultaneous absorption of $\lambda\mathcal{N}$ photons with GDR energy. This process is very different from the absorption of a single photon with $\mathcal{N}$-times the GDR energy. The obvious reason is that such photon can only be absorbed by a pair of nucleons due to its small momentum, whereas the multiphonon states are very collective, involving all nucleons in the nucleus due to the long wavelength of the photons absorbed. It would be necessary a very intense photon beam, up to now inexistent, in order to excite such states in photo-induced reactions. The Coulomb field of heavy ions seem to be the only available source to achieve such states.

It should be pointed out that resonance-like structures have already been observed in peripheral heavy-ion collisions at intermediate energies [29]) and have been interpreted [30]) as due to multiple excitation of giant resonances of different multipolarity. In contrast to the high energy case, the predominant agent at intermediate energies is the nuclear interaction in grazing collisions. Albeit such studies, very little is known about the multiphonon states, especially concerning their decay mechanism. At the present stage it is presumably much more important to obtain signatures of the existence of such states in high energy collisions, what would complement the experimental information from intermediate energy collisions.

Based on these arguments, we make the basic assumption that the multiphonon states couple to the compound nucleus states, which decay statistically. The decay modes of the compound states were calculated by using the code ALICE/LIVERMORE/85/300 [31]). The code has as input parameters the inverse reaction cross sections, level densities, etc. established in a global set as in ref. [32]). It has been developed in order to describe nuclear fusion reactions, but the decay modes of the residual compound nucleus are independent of the entrance reaction channel. A neutron-induced reaction was simulated in order to reproduce an excited compound nucleus with the energy $E_{\mathcal{N}} = \mathcal{N}\hbar\omega_{\mathrm{GDR}}$. As the excitation of multiphonon states brings in negligible angular momentum - see ref. [17]) for a study of the angular momentum probabilities in multiphonon excitations - the angular momentum dependence of the formation process was neglected.

For each multiphonon state $\mathcal{N}$, this procedure allowed us to determine the decay probabilities $C_\alpha^{\mathcal{N}}$ for a particular channel α. The reaction probability for a specific fragmentation channel in a RHI collision is given by

$$\mathcal{P}_\alpha(b) = \sum_{\mathcal{N}} C_\alpha^{\mathcal{N}} P_{\mathcal{N}}(b), \tag{3.10}$$

where $P_{\mathcal{N}}(b)$ is given by (3.1). The total cross section for relativistic Coulomb fragmentation of heavy ions into the channel α is obtained by an integration of (3.10) over impact parameters from the minimum grazing value, i.e.,

$$\sigma_\alpha = 2\pi \int_{R_{\mathrm{P}}+R_{\mathrm{T}}}^{\infty} b\mathcal{P}_\alpha(b)\,\mathrm{d}b. \tag{3.11}$$

In tables 1 and 2 we present the experimental data from refs. [2,5]) on the electromagnetic cross sections for the removal of one and two neutrons in RHI collisions. Also shown are the numerical results obtained with the procedure described above. We see that the agreement with the experimental data is surprisingly good, despite all simplifying assumptions used in the theory. These results are essentially equal to the ones obtained with the equivalent photon method [1-15]), by means of a folding of the equivalent photon numbers and the $\sigma(\gamma, \mathrm{n})$ and $\sigma(\gamma, 2\mathrm{n})$ photo cross sections. Therefore, it is not possible to have a signature from these data of any process which cannot be attributed to the well known (single) excitation by means of real

TABLE 1

Cross sections for one-neutron removal reactions due to relativistic Coulomb excitation

Reaction	Energy (GeV/nucleon)	Measured cross section (b)	Calculated cross section (b)
^{197}Au(^{12}C, X)^{196}Au	2.1	0.075 (14)	0.051
^{197}Au(^{20}Ne, X)^{196}Au	2.1	0.153 (18)	0.141
^{197}Au(^{40}Ar, X)^{196}Au	1.8	0.348 (34)	0.396
^{197}Au(^{56}Fe, X)^{196}Au	1.7	0.601 (54)	0.625
^{197}Au(^{139}La, X)^{196}Au	1.26	1.97 (13)	2.03
^{197}Au(^{238}U, X)^{196}Au	0.96	5.3 (5) [a]	4.50
^{59}Co(^{12}C, X)^{58}Co	2.1	0.006 (9)	0.008
^{59}Co(^{20}Ne, X)^{58}Co	2.1	0.032 (11)	0.022
^{59}Co(^{56}Fe, X)^{58}Co	1.7	0.088 (14)	0.133
^{59}Co(^{139}La, X)^{58}Co	1.26	0.28 (4)	0.320
^{16}O(^{197}Au, X)^{196}Au	60	0.280 (30)	0.244
^{16}O(^{197}Au, X)^{196}Au	200	0.440 (40)	0.326

[a]) Preliminary results.

photons. Moreover, the cross section (3.11) is dominated by the single step ($\mathcal{N}=1$) process for the one- or two-neutron emission channels, as can be attested from fig. 8 where the total cross section for the relativistic Coulomb excitation of multiphonon states in ^{197}Au targets by means of ^{139}La projectiles are displayed. These cross sections were obtained by adding up the contributions of all decay channels subsequent to the excitation of a given multiphonon state $\mathcal{N}$, i.e.,

$$\sigma_{\mathcal{N}} = 2\pi \int_{R_P+R_T}^{\infty} bP_{\mathcal{N}}(b)\,\mathrm{d}b\,. \tag{3.12}$$

TABLE 2

Cross sections for two-neutron removal reactions due to relativistic Coulomb excitation, in milibarns

Reaction	Energy (GeV/nucleon)	Measured cross section (mb)	Calculated cross section (mb)
^{197}Au(^{12}C, X)^{195}Au	2.1	9 (17)	3
^{197}Au(^{20}Ne, X)^{195}Au	2.1	49 (15)	19
^{197}Au(^{40}Ar, X)^{195}Au	1.8	76 (18)	56
^{197}Au(^{56}Fe, X)^{195}Au	1.7	73 (13)	80
^{197}Au(^{139}La, X)^{194}Au	1.26	335 (49)	263
^{59}Co(^{12}C, X)^{57}Co	2.1	6 (4)	1.2
^{59}Co(^{20}Ne, X)^{57}Co	2.1	3 (5)	3.2
^{59}Co(^{56}Fe, X)^{57}Co	1.7	13 (6)	16
^{59}Co(^{139}La, X)^{57}Co	1.26	32 (16)	37

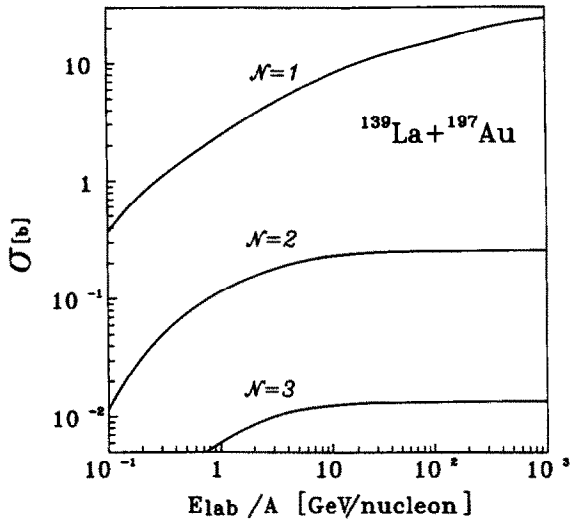

Fig. 8. Cross sections for the excitation of multiphonon states in ^{197}Au for the reaction ^{139}La+^{197}Au as a function of the laboratory energy per nucleon.

The total cross section for RHI Coulomb excitation, $\sigma = \sum_{\mathcal{N}} \sigma_{\mathcal{N}}$ depends on the projectile charge as $Z_P^{1.7-1.9}$, in contrast to what is expected from the Z_P^2 law, characteristic from a single (direct) step process. A clue on the existence of multiphonon states could be obtained by an accurate experimental measurement of this dependence.

Certainly, the most indicative signature of a multiphonon excitation is the emission of heavier particles. In experiments with very heavy nuclei, the measurement of fission cross sections may be a possible signature. Let us take ^{232}Th as an example. The photo-fission cross section $\sigma(\gamma, \mathrm{F})$ has been measured in several experiments [see, e.g., ref. [35]) for $E_\gamma = 15$–104 MeV]. If the relativistic Coulomb excitation proceeds only via a single step, the fission cross sections can be calculated, with a good accuracy, in the equivalent photon method (EPM), i.e.,

$$\sigma_F^{EPM} = \int \frac{dE_\gamma}{E_\gamma} n(E_\gamma)\sigma(\gamma, \mathrm{F}) , \tag{3.13}$$

where $\sigma(\gamma, \mathrm{F})$ is the photo-fission cross section for the photon energy E_γ, and $n(E_\gamma)$ is the equivalent photon number given analytically in e.g. ref. [11]) [see also ref. [1])]. On the other hand, if multiple excitation of giant resonances is accessible in RHI collisions, the cross sections for the fission channel, σ_F, may be calculated by means of (3.10) and (3.11). In fig. 9 we plot the ratio σ_F/σ_F^{EPM} for the reaction ^{232}Th+^{232}Th as a function of the laboratory energy. The $\sigma(\gamma, \mathrm{F})$ cross sections and the fission probabilities $C_F^{\mathcal{N}}$ in (3.10) were taken from literature [33-35]). One observes that both calculations give nearly the same results for $E_{lab} < 1$ GeV/nucleon but they differ

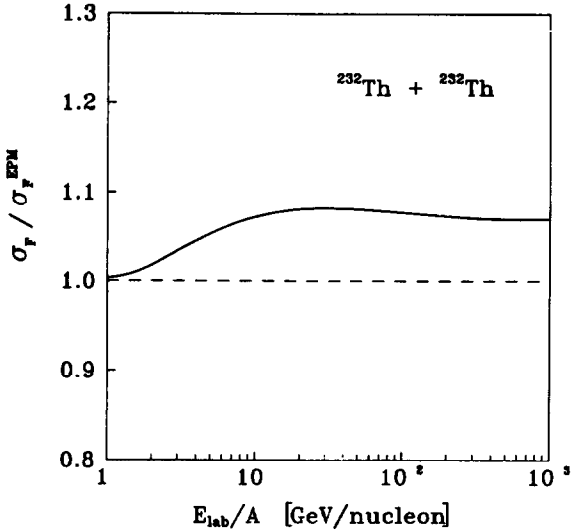

Fig. 9. Ratio of the fission cross sections for ^{232}Th nuclei in the reaction ^{232}Th + ^{232}Th calculated under the assumptions of multiple GDR excitation, σ_F, and within the equivalent photon method, σ_F^{EPM}, which presupposes a direct step process.

by 10% for very high energies, with the fission cross sections being higher if they proceed via multiphonon excitation. This discrepancy should be even larger due to the following reasoning. The fission probabilities $C_F^{\mathcal{N}}$ do not correspond to the actual decay probabilities of multiphonon states, but to those induced by real photons with energies $E_\gamma = \mathcal{N}\hbar\omega_{GDR}$. It is found experimentally that the fission probability of ^{232}Th is about 18%, 40% and 60% for $E_\gamma = 15$, 30 and 45 MeV, respectively [35]). But, due to the large amplitude collective motion of a multiphonon state, the fission probability for $\mathcal{N} = 2, 3, \ldots$ is expected to be bigger than the values given above. Therefore, the existence of multiphonon states would lead to an enhancement of the total fission cross section, not compatible with the equivalent photon approximation.

5. Conclusions

The hydrodynamical model for collective vibrations of protons against neutrons in nuclei is shown to be very appropriate for an investigation of the consequences of relativistic Coulomb excitation of heavy ions. There are strong evidences that states higher in energy than the usual giant dipole resonances may be reached. By means of a simple harmonic model for the giant dipole vibrations it was possible to infer the probabilities and cross sections for the excitation of such states. Assuming that there will be a complete mixing of the multiphonon states with the underlying compound nucleus states, predictions about the decay modes of these states were performed.

However, it must be borne in mind that our calculations are essentially schematic. The obvious reason is that the characteristics of the multiphonon states are completely unknown. It is not even clear if they exist at all. In this sense the calculations performed in this article may help to plan future experiments.

The coherent action of the electromagnetic field of a periodic string of nuclei in a crystal [36]) is a promising tool to investigate the response of nuclei to a very collective dipole motion never investigated before, and only accessible by means of this mechanism.

The authors are very grateful to T. Kodama and J.C. Hill for stimulating discussions and to M. Blann for helping us with the ALICE code. This work was supported in part by CNPq/Conselho Nacional de Desenvolvimento Científico e Tecnológico and by FAPERJ/Fundação de Amparo à Pesquisa do Estado do Rio de Janeiro.

References

1) C.A. Bertulani and G. Baur, Phys. Reports **163** (1988) 299
2) J.C. Hill, Proc. Int. Workshop on relativistic aspects of nuclear physics, Rio de Janeiro, September 1989, ed. T. Kodama *et al.* (World Scientific, Singapore)
3) H.H. Heckman and P.J. Lindstron, Phys. Rev. Lett. **37** (1976) 56
4) M.T. Mercier *et al.*, Phys. Rev. Lett. **52** (1984) 898; Phys. Rev. **C33** (1986) 1655
5) J.C. Hill *et al.*, Phys. Rev. Lett. **60** (1988) 999
6) C. Brechtmann and W. Heinrich, Z. Phys. **A331** (1988) 463
7) C. Brechtmann, W. Heinrich and E.V. Benton, Phys. Rev. **C39** (1989) 2222
8) J. Barrette *et al.*, Phys. Rev. C, submitted
9) C.A. Bertulani and G. Baur, Nucl. Phys. **A458** (1986) 725
10) J.W. Norbury, Phys. Rev. **C41** (1990) 372
11) J.D. Jackson, Classical electrodynamics (Wiley, New York, 1975);
C.A. Bertulani and G. Baur, Nucl. Phys. **A442** (1985) 739
12) J.W. Norbury, Phys. Rev. **C39** (1989) 2472; **C40** (1989) 2621
13) A. Winther and K. Alder, Nucl. Phys. **A319** (1979) 518
14) C.A. Bertulani and G. Baur, Phys. Rev. **C33** (1986) 910
15) R. Fleischhauer and W. Scheid, Nucl. Phys. **A493** (1989) 583
16) D. Lissauer *et al.*, "Study of extreme peripheral to central collisions in reactions induced by relativistic heavy ions, Proposal for AGS experiment 814, Brookhaven National Laboratory, 1985
17) G. Baur and C.A. Bertulani, Phys. Lett. **B174** (1986) 23; Phys. Rev. **C34** (1986) 1654
18) W.D. Myers, W.J. Swiatecki, T. Kodama, L.J. El-Jaick and E.R. Hilf, Phys. Rev. **C15** (1977) 2032
19) B.L. Berman, At. Data Nucl. Data Tables **15** (1975) 319
20) J. Ahrens *et al.*, Proc. Int. Conf. on photonuclear reactions and applications, Asilomar, 1973, ed. B.L. Berman (LBL, Univ. of California, 1973)
21) B.L. Berman and S.C. Fultz, Rev. Mod. Phys. **47** (1975) 713
22) B.L. Berman, B.F. Gibson and J.S. O'Connell, Phys. Lett. **B66** (1976) 405
23) E. Merzbacher, Quantum mechanics, 2nd ed. (Wiley, New York, 1970)
24) A.S. Goldhaber, Phys. Lett. **B53** (1974) 306
25) G.F. Bertsch, Phys. Rev. Lett. **46** (1981) 472
26) M.J. Murphy, Phys. Lett. **B135** (1984) 25
27) H.H. Gan, S.J. Lee, S. Das Gupta and J. Barrete, Phys. Lett. **B234** (1990) 4
28) J.S. Levinger, Phys. Rev. **84** (1951) 43
29) N. Frascaria *et al.*, Phys. Rev. Lett. **39** (1977) 918

30) Ph. Chomaz and D. Vautherin, Phys. Lett. **B139** (1984) 244;
Ph. Chomaz, Nguyen Van Giai and D. Vautherin, Nucl. Phys. **A476** (1988) 125
31) M. Blann and J. Bisplinghoff, Lawrence National Laboratory Report UCID-19614 (1982) unpublished
32) M. Blann and H.K. Vonach, Phys. Rev. **C28** (1983) 1475
33) A. Veyssière *et al.*, Nucl. Phys. **A199** (1973) 45
34) J.T. Caldwell *et al.*, Phys. Rev. **C21** (1980) 215
35) A. Lepetre *et al.*, Nucl. Phys. **A472** (1987) 533
36) Yu.L. Pivovarov, A.A. Shirokov and S.A. Vorobiev, Nucl. Phys. **A509** (1990) 800